Direct Observation of Quasi-Bound States and Band-Structure Effects in a Double Barrier Resonant Tunneling Structure Using Ballistic Electron Emission Microscopy

T. Sajoto,[1] J. J. O'Shea,[2] S. Bhargava,[1] D. Leonard,[2] M. A. Chin,[1] and V. Narayanamurti[1]

[1]*Electrical and Computer Engineering Department, University of California, Santa Barbara, California 93106*

[2]*Materials Department, University of California, Santa Barbara, California 93106*

(Received 15 August 1994)

Ballistic electron emission microscopy (BEEM) has been used to study transport in a double barrier resonant tunneling structure. Unlike conventional transport techniques, BEEM allows the injected electron energy to be varied *independent* of the band profile. We report the observation of quasi-bound states and band-structure effects as deduced from the temperature evolution of the BEEM spectra. The BEEM thresholds are found to be in good agreement with the calculated energetically favorable levels. Our results show that BEEM is a powerful spectroscopic tool for studying quantum structures.

PACS numbers: 73.20.At, 61.16.Ch, 73.40.Gk, 73.40.Kp

The advent of nanogrowth and nanolithography techniques such as molecular-beam epitaxy (MBE) and electron-beam lithography has opened up new research frontiers in the studies of novel quantum phenomena. Recently invented nanospectroscopy techniques such as scanning-tunneling microscopy (STM) [1,2] and ballistic electron emission microscopy (BEEM) [3] should further shed light in answering some of the unresolved fundamental issues related to the growth, fabrication, and characterization of quantum devices.

Kaiser and Bell [3] first demonstrated the unique capability of BEEM not only to perform microscopy studies with nanometer resolution, but also to spectroscopically probe metal/semiconductor (M/S) interfaces on a *local* scale. The invention of BEEM has fueled a great deal of research activities, the majority of which have focused on the studies of charge transport across M/S interfaces [4–9]. Henderson *et al.* [10] theoretically predicted the observation of electron wave interference effects using BEEM. Recently, Kaiser *et al.* [11] reported BEEM studies of AlAs on GaAs. However, the potential of using BEEM as a powerful spectroscopic tool to study charge transport across *spatially buried* quantum structures has not been fully explored.

In this Letter, we show that BEEM can be used to study transport in a *buried* double barrier resonant tunneling structure (DBRTS) [12]. We have also shown that BEEM can be used to measure the band offset in *buried* single barrier $Al_xGa_{1-x}As/GaAs$ heterojunctions [13]. The presence of bias-induced band bending in a two-terminal current-voltage measurement complicates the self-consistent analysis of the charge transport and leads to an uncertainty for converting the applied voltage to an energy scale [14,15]. BEEM, on the other hand, allows the injected electron energy to be varied *independent* of the band profile. Hence, BEEM can be expected to provide a more direct determination of the energy levels. The energetically favorable states in the higher-lying valleys can also be readily probed by BEEM. We report the observation of quasi-bound states (QBS's) and band-structure effects in the DBRTS as deduced from the systematic temperature (T) evolution of the BEEM spectra. A more detailed account of this work will be published elsewhere.

The DBRTS was grown by MBE on an n^+-GaAs(100) substrate and is schematically shown in the inset to Fig. 1. Several noteworthy design parameters are as follows. First, a p-type (Be) δ-doping sheet with the appropriate doping concentration was inserted between the GaAs buffer and spacer layers to flatten the band to enable us to obtain a direct measurement of the energy levels [16]. The GaAs buffer, spacer, and cap layers were designed to be thin enough to allow the injected electrons to be collected. The GaAs spacer layer was also designed to be thick enough to prevent diffusion of the Be δ-doping sheet into the AlGaAs barriers and GaAs quantum well (QW) to minimize impurity scattering. The AlGaAs barriers were designed to be thin enough to allow tunneling of the injected electrons, yet thick enough to compensate for possible growth parameter uncertainties. The GaAs QW was designed to allow for the observation of one QBS_Γ in the Γ-band QW and to compensate for growth parameter uncertainties.

The base layer was obtained by evaporating 100 Å of Au. The measurements were performed in a Surface/Interface AIVTB-4 BEEM/STM using a Au tip in ambient atmosphere and liquid nitrogen [17]. The tip-base voltage (V) was varied between 0.7 and 1.7 V to acquire the collector current (I_C) while maintaining a constant tunneling current (I_t) of 2 nA. Spectra consisting of at least 500 bias points (2 meV/point) were acquired to allow for subsequent numerical data processing. The spectra were typically averaged for 25–100 tip-base voltage scans (4 sec/scan) to improve the signal-to-noise ratio. The raw BEEM I_C-V spectrum was first smoothed and then numerically differentiated with a 10 meV window to obtain the first derivative (dI_C/dV-V). The dI_C/dV-V was then smoothed and numerically differentiated again with a 10 meV window to obtain the second derivative (d^2I_C/dV^2-V). The variation in the BEEM thresholds

(V_T's) from scan to scan ($\leq \pm 20$ meV), which is determined mainly by the drift and the spatial variation of the *local* potential profile of the sample, sets an experimental limit on the lowest measurable energy level separation that can be obtained with BEEM. This limit is in addition to the energy resolution limit set by the width of the injected electron energy distribution.

Figure 1 shows the Γ conduction band-edge ($E_{c,\Gamma}$) profile for the DBRTS at 77 K. The band profile and QBS_Γ were obtained by solving the Poisson and Schrödinger equations with two assumptions [16]. First, $E_{c,\Gamma}$ of the GaAs cap layer at the M/S interface was assumed to be 0.99 eV above the Fermi level (E_F), as determined experimentally [13]. Second, we used the effective masses, band gaps, and other parameters in Ref. [18] and assumed that the Γ conduction band-edge discontinuity ($\Delta E_{c,\Gamma}$) is 62% of the Γ band-gap difference ($\Delta E_{g,\Gamma}$). The QBS_Γ was designed to be sufficiently higher than $E_{c,\Gamma}$ of the GaAs cap layer at the M/S interface to ensure that the first threshold (V_{TA}) associated with tunneling through the QBS_Γ will be observed despite the possible presence of a small band bending (due to the growth parameter uncertainties or T change). The band bending changes mainly because the M/S Schottky barrier (Φ_{Bn}) increases from $\approx$0.90 to $\approx$0.99 eV as T decreases from 300 to 77 K.

To ensure that V_{TA} is a true signature of tunneling through the QBS_Γ, two additional reference samples (AL0.0 and AL0.42) were studied. The structures of both samples are similar to that of the DBRTS except that the GaAs QW and AlGaAs barriers were replaced by a 100 Å GaAs layer for AL0.0 and a 100 Å single $Al_{0.42}Ga_{0.58}As$ barrier for AL0.42. Unlike the barriers in the DBRTS, the barrier in AL0.42 was designed to be thick enough to prevent appreciable tunneling of the injected electrons with energy lower than the barrier height. It is clear that if resonant transmission occurs, then V_{TA} of the DBRTS should lie between the V_{TA}'s of the AL0.0 and AL0.42.

Figure 2 shows three different BEEM spectra for the AL0.0, DBRTS, and AL0.42. Three striking observations can be made. First, V_{TA} of the DBRTS is lower than V_{TA} of the AL0.42, which has the same barrier *height* of $Al_{0.42}Ga_{0.58}As$. Second, V_{TA} of the DBRTS is in good agreement with the calculated QBS_Γ. In addition, V_{TA}'s of the AL0.0 and AL0.42 are also in good agreement with the expected energy for conduction over the $E_{c,\Gamma}$ of GaAs and $E_{c,\Gamma}$ of $Al_{0.42}Ga_{0.58}As$, respectively [13]. These observations are direct evidence of resonant transmission through the QBS_Γ. The position of the QBS_Γ with respect to the bottom of the QW and the conduction band offset for the $Al_{0.42}Ga_{0.58}As$ barrier can be deduced from the differences between V_{TA} of the DBRTS and V_{TA} of AL0.0, and between V_{TA} of AL0.42 and V_{TA} of AL0.0, respectively. Assuming that there is no uncertainty in the growth parameters, the correction due to band bending is small ($\sim$10 meV) at 77 K. Finally, the I_C-V line shapes are strikingly different. For AL0.0 and AL0.42, the additional features in the I_C-V for $V > V_{TA}$ can be attributed to the opening of additional conduction channels associated with the higher-lying L and X valleys.

Figure 3 shows the calculated $E_{c,\Gamma}$, $E_{c,L}$, and $E_{c,X}$ band profiles as well as the various QBS's in the QW's at 77 K. For the Γ and L bands, we have a DBRTS with one QBS_Γ and one QBS_L, respectively. For the X band, however, we have coupled double QW's with two degenerate QBS_{X1} and QBS_{X2}, and another QBS_{X3}.

To date, various models [4–9] have been used to fit the I_C-V to extract the V_T's and to elucidate the underlying transport processes. However, it is also important to be able to extract the V_T's experimentally to complement the theoretical curve fitting. This becomes evident in the case of the DBRTS where modeling the multivalley conduction would require a complicated self-consistent fitting procedure using a considerable number of adjustable parameters. The experimental extraction of V_T's using the derivative technique is not model dependent and does not require adjustable parameters or *a priori* knowledge of the band-structure parameters. The complex nature of the scattering processes as well as the energy and momentum conservation conditions involving the different bands in our case are presently not well understood. Although

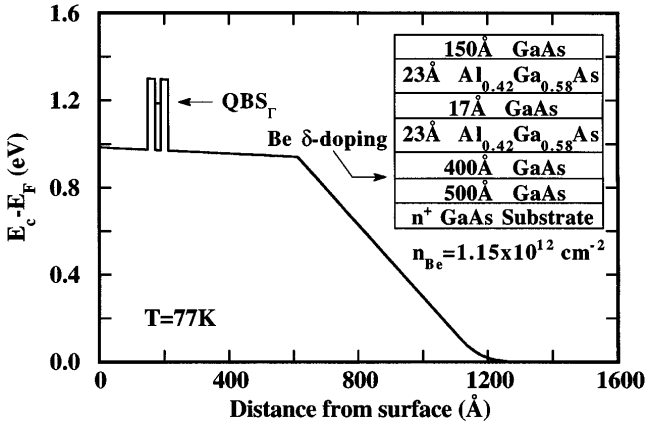

FIG. 1. DBRTS band profile at 77 K. The inset shows the sample structure.

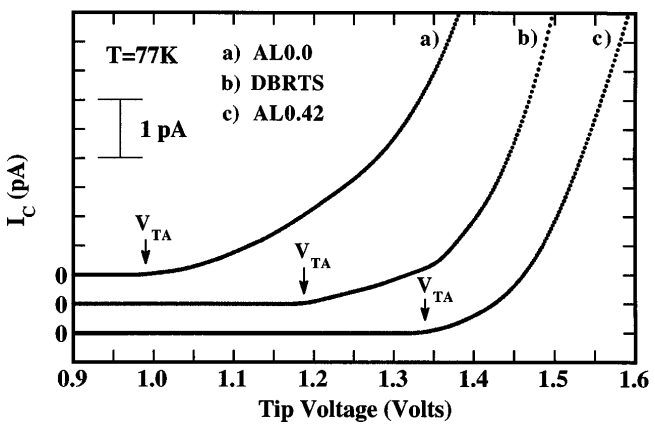

FIG. 2. BEEM I_C-V spectra at 77 K for (a) AL0.0, (b) DBRTS, and (c) AL0.42.

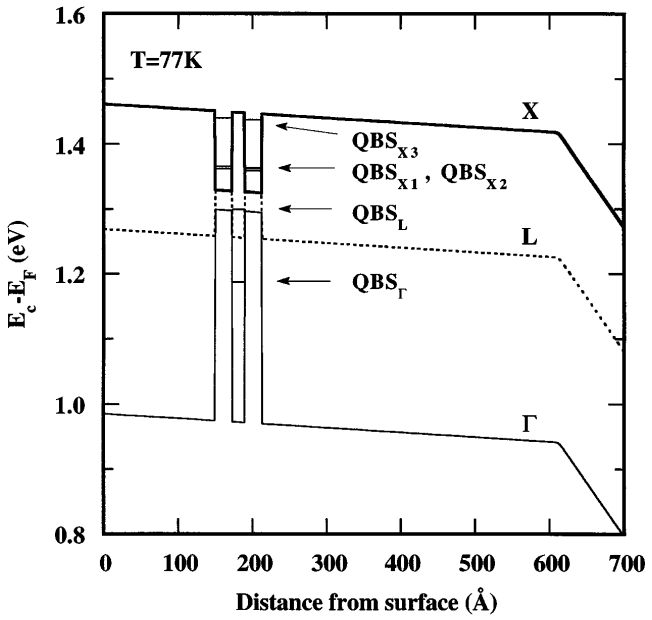

FIG. 3. DBRTS band profiles and QBS's for the Γ, L, and X bands at 77 K.

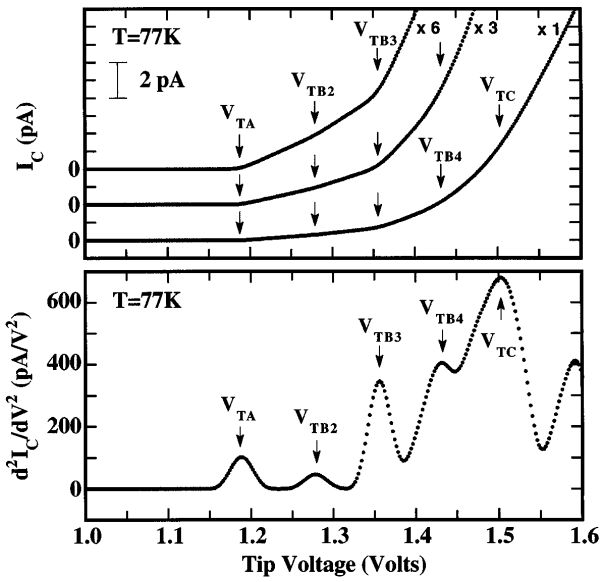

FIG. 4. I_C-V and d^2I_C/dV^2-V for the DBRTS at 77 K. The I_C-V is magnified to clearly show the presence of additional structures beyond V_{TA}. The peaks in the d^2I_C/dV^2-V correspond to the V_T's in the I_C-V.

energy and transverse momentum conservations are generally assumed, various features in the BEEM spectrum which contradict these assumptions were also observed [4,9,11].

We have therefore decided to focus on the analysis of the T dependence of the BEEM spectra. The structures in the I_C-V can be attributed to the openings of additional conduction channels. Figure 4 shows the I_C-V and d^2I_C/dV^2-V at 77 K. The I_C-V is magnified to show the presence of additional structures beyond V_{TA}. The I_C-V from below threshold up to the first (V_{TA}), second (V_{TB2}), and third (V_{TB3}) thresholds at low T can be qualitatively approximated by piecewise linear segments with the V_T's corresponding to the intersections between two consecutive line segments (the kinks in the I_C-V). The peaks in the d^2I_C/dV^2-V should then correspond to the positions of the V_T's in the I_C-V. The deviation from linearity results in the broadening of the d^2I_C/dV^2-V peaks as well as the nonzero amplitudes of the d^2I_C/dV^2-V valleys.

Figure 5 shows the systematic T evolution of d^2I_C/dV^2-V. The salient features of the T dependence are as follows. First, as T decreases from 300 to 77 K, the peaks in the d^2I_c/dV^2-V (i.e., V_T's) move to higher values as expected, since the energy gaps of both GaAs and AlGaAs increase as T decreases. Second, as T decreases, the structures become more pronounced and narrower, and additional structures are clearly observed. The second threshold at high T (V_{TB}) gradually splits into three peaks: V_{TB2}, V_{TB3}, and V_{TB4}. This is consistent with the reduction in the thermally activated scattering processes as well as the narrowing of the Fermi-Dirac distribution of the injected electron energy.

Figure 6 shows the T dependence of the calculated energy levels (QBS$_\Gamma$, QBS$_L$, $E_{c,\Gamma\text{-max}}$ and $E_{c,L\text{-max}}$ of the AlGaAs barriers, QBS$_{X1\text{-max}}$, QBS$_{X2\text{-max}}$, QBS$_{X3\text{-max}}$, and $E_{c,X\text{-max}}$ for GaAs as shown in Fig. 3) and the observed V_T's deduced from the peaks of the d^2I_C/dV^2-V (V_{TA}, V_{TB}, V_{TB2}, V_{TB3}, V_{TB4}, and V_{TC} in Fig. 5). The error bar is mainly due to the spatial variation of the potential profile and the drift. We assumed that the increase in Φ_{Bn} from $\approx$0.90 eV (300 K) to $\approx$0.99 eV (77 K) follows the same T dependence as the GaAs Γ band

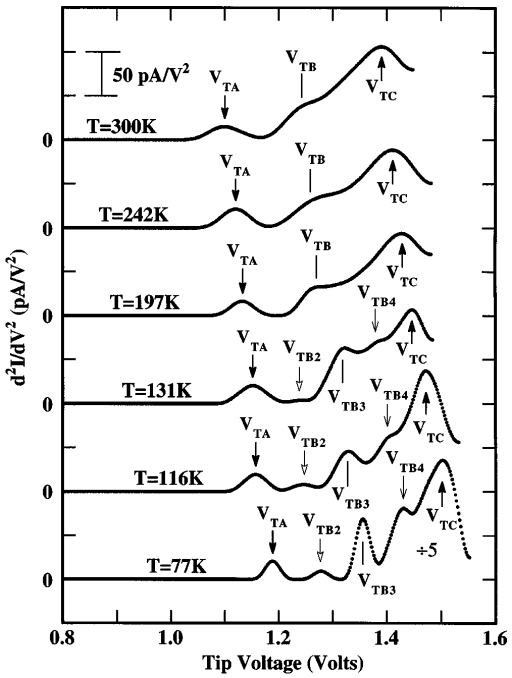

FIG. 5. Systematic T evolution of d^2I_C/dV^2-V.

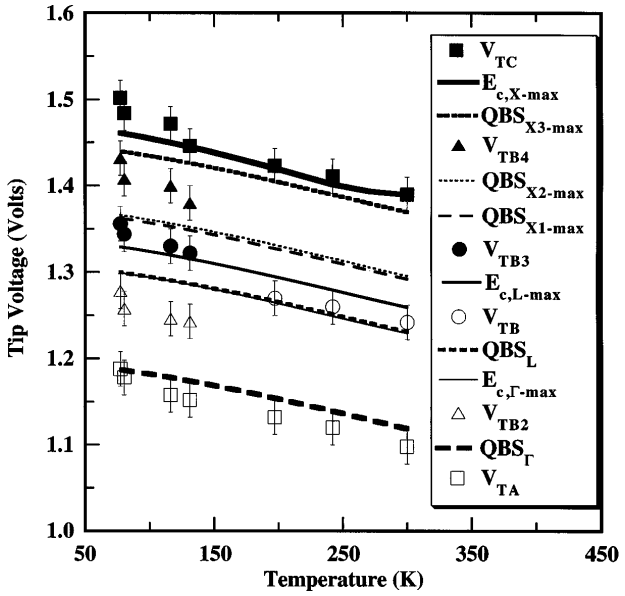

FIG. 6. T dependence of the calculated energetically favorable levels (see Fig. 3) and the observed V_T's deduced from the peaks of the d^2I_C/dV^2-V in Fig. 5. Solid lines correspond to the band edges, whereas dashed (dotted) lines correspond to the QBS's.

gap [18]. The conduction process we envision here is due to the summation of conduction through the Γ, L, and X transmission channels with some interband couplings [19,20]. The L and X states scatter into the Γ propagating states before being collected at the collector. The measured V_T's are in good agreement with the calculated energy levels. The discrepancy could be accounted for if the δ-doping concentration is lower by $\sim$15%. The calculated energy levels would then be lowered by $\sim$20 meV, but the good fit for $E_{c,X\text{-max}}$ would not be affected.

We attribute V_{TA} to tunneling through the QBS_Γ. At higher T, the broad V_{TB} peak corresponds to the *collective* contribution of tunneling through the QBS_L and injection over the $E_{c,\Gamma\text{-max}}$ and $E_{c,L\text{-max}}$ of the AlGaAs barriers. The presence of quantum mechanical reflection increases the V_T associated with injection over the AlGaAs barriers. V_{TB2} can be attributed to tunneling through the QBS_L and the finite probability of transmission across the $E_{c,\Gamma\text{-max}}$ of the AlGaAs barriers. V_{TB3} can be attributed to injection over the $E_{c,\Gamma\text{-max}}$ and $E_{c,L\text{-max}}$ of the AlGaAs barriers as well as tunneling through QBS_{X1} and QBS_{X2}. V_{TB4} can be attributed to tunneling through the QBS_{X3}. Finally, V_{TC} can be attributed to the conduction through the X valley of the GaAs.

In summary, we have shown, for the first time, that BEEM can be used as a powerful spectroscopic tool to study quantum transport in a DBRTS *spatially buried* beneath the Schottky barrier. The V_T's and their T evolution are found to be in good agreement with the calculated energetically favorable levels. We have shown that BEEM can potentially be used to study charge transport in low-dimensional quantum structures such as quantum wires and quantum dots. The invaluable understanding regarding the transport processes can then be used to exploit the quantum nature of charge transport and to improve future generations of novel quantum devices.

We thank W. J. Kaiser, M. H. Hecht, L. D. Bell, and S. J. Manion of the Jet Propulsion Laboratory as well as C. E. Bryson and M. Ackeret of Surface/Interface, Inc. for sharing their considerable BEEM expertise. We acknowledge discussions with I. H. Tan, Y. P. Li, and J. P. Ibbetson. The BEEM facility at UCSB was set up under a UC/MICRO grant and a CalTech President's Award. This work was supported by NSF under Grants No. DMR-9313610 and No. DMR-912007, and AFOSR under Grant No. F49620-94-1-0378.

[1] G. Binnig, H. Rohrer, Ch. Gerber, and E. Weibel, Phys. Rev. Lett. **49**, 57 (1982).
[2] P. Muralt, H. Meier, D. W. Pohl, and H. W. Salemink, Appl. Phys. Lett. **50**, 1352 (1987).
[3] W. J. Kaiser and L. D. Bell, Phys. Rev. Lett. **60**, 1406 (1988).
[4] L. D. Bell and W. J. Kaiser, Phys. Rev. Lett. **61**, 2368 (1988).
[5] M. Prietsch and R. Ludeke, Phys. Rev. Lett. **66**, 2511 (1991).
[6] L. J. Schowalter and E. Y. Lee, Phys. Rev. B **43**, 9308 (1991).
[7] H. D. Hallen, A. Fernandez, T. Huang, J. Silcox, and R. A. Buhrman, Phys. Rev. B **46**, 7256 (1992).
[8] G. N. Henderson, P. N. First, T. K. Gaylord, and E. N. Glytsis, Phys. Rev. Lett. **71**, 2999 (1993).
[9] R. Ludeke and A. Bauer, Phys. Rev. Lett. **71**, 1760 (1993).
[10] G. N. Henderson, T. K. Gaylord, E. N. Glytsis, P. N. First, and W. J. Kaiser, Solid State Commun. **80**, 591 (1991).
[11] W. J. Kaiser, M. H. Hecht, L. D. Bell, F. J. Grunthaner, J. K. Liu, and L. C. Davis, Phys. Rev. B **48**, 18 324 (1993).
[12] A preliminary account of this work was presented at the Fifth Annual BEEM Workshop, Mohonk, New York, 24 January 1994; see Proceedings of the BEEM'94 Conference, pp. 6–8.
[13] J. J. O'Shea, T. Sajoto, S. Bhargava, D. Leonard, M. A. Chin, and V. Narayanamurti, J. Vac. Sci. Technol. B **12**, 2625 (1994).
[14] L. L. Chang, L. Esaki, and R. Tsu, Appl. Phys. Lett. **24**, 593 (1974).
[15] V. J. Goldman, D. C. Tsui, and J. E. Cunningham, Phys. Rev. B **35**, 9387 (1987).
[16] G. L. Snider, 1D Poisson-Schrödinger Solver version 1.1.10d.
[17] Surface/Interface, Inc., Mountain View, CA 94041.
[18] S. Adachi, J. Appl. Phys. **58**, R1 (1985).
[19] C. Mailhiot, T. C. McGill, and J. N. Schulman, J. Vac. Sci. Technol. B **1**, 439 (1983).
[20] T. Ando and H. Akera, Phys. Rev. B **40**, 11 619 (1989).